Original

Dieringa, H.; Hort, N.; Kainer, K.U.:

Microstructure and Compression Creep Strength of the Newly Developed Magnesium Alloy DieMag422

Advanced Materials Research, AMI Light Metals Conference 2014 (2014)
Trans Tech Publications

DOI: 10.4028/www.scientific.net/AMR.891-892.1457

Advanced Materials Research
ISSN: 1662-8985, Vol. 1019, pp 177-183
doi:10.4028/www.scientific.net/AMR.1019.177

Submitted: 2014-05-06
Revised: 2014-05-22
Accepted: 2014-05-22
Online: 2014-10-20

Microstructure and Compression Creep Strength of the Newly Developed Magnesium Alloy DieMag422

DIERINGA Hajo [a *], HORT Norbert [b] and KAINER Karl Ulrich [c]

Helmholtz-Zentrum Geesthacht, MagIC – Magnesium Innovation Centre

21502 Geesthacht, Germany

[a]hajo.dieringa@hzg.de, [b]norbert.hort@hzg.de, [c]karl.kainer@hzg.de

Keywords: Creep Resistance, Precipitation Strengthening, Barium, Calcium, Die Casting

Abstract. Magnesium alloys have been finding increasingly more types of application in the automotive and aerospace industries for over twenty years. Despite the fact conventional magnesium alloys have limited high-temperature strength and creep resistance, especially when they contain aluminium as an alloying element. Aluminium is necessary to improve the castability when high-pressure die casting is the favoured process. Applications with higher operating temperatures require additional alloy elements, which form precipitates with the aluminium during solidification and therefore prevent the formation of $Mg_{17}Al_{12}$, which is responsible for the low creep resistance of magnesium alloys that contain aluminium. The precipitates formed may also strengthen grain boundaries and so improve the creep strength. Barium and calcium were investigated as elements in a magnesium alloy containing aluminium (DieMag422: 4 wt.-% Al, 2 wt.-% Ba, 2 wt.-% Ca). The compression creep strength was compared at 240°C for stresses between 60 and 120 MPa with two commercial creep-resistant magnesium alloys, AE42 and MRI230D. The stress exponents were calculated from the stress dependence of the minimum creep rate. The concept of a threshold stress was applied and true stress exponents n_t close to 5 were found. The new alloy DieMag422 exhibits improved creep strength compared to both commercial alloys and also has proven it is die castable.

Introduction

The stability of magnesium alloys at higher temperatures remains an aim in the field of research into magnesium based materials. Alloys containing rare earth elements are commercially available and show a satisfying creep resistance, such as AE42 and AE44. Due to the limited availability of rare earth elements, the price of these alloying elements varies and is uncertain. The avoidance of such elements is therefore desirable. Calcium and strontium are alkaline earth elements found in the second column of the periodic table of elements. Both improve the creep resistance magnesium alloys containing aluminium that are used for high-pressure die casting (HPDC). Barium, as another element in the second column, would likely have chemically similar advantages and due to having an atomic radius 1.36 times larger than magnesium could aid solid solution strengthening. Binary Mg-Ba phases ($Mg_{17}Ba_2$, $Mg_{23}Ba_6$ and Mg_2Ba) have been reported [1-5], as well as Al-Ba phases (AlBa, Al_2Ba, Al_4Ba, $Al_{13}Ba_7$, Al_5Ba_4) [6-12]. The chemical affinity of aluminium to additional alloying elements is important as the formation of $Mg_{17}Al_{12}$ β-phase may be prohibited, because any free aluminium is attracted by the calcium or barium. The β-phase is known to deteriorate the creep resistance of magnesium alloys [13, 14], such as AZ91 and AM50/60, but the aluminium is necessary for its ability to permit high-pressure die casting for room temperature applications like steering wheels and seat frames.

Experimental

Magnesium alloy DieMag422 was mixed from a melt containing very pure magnesium (> 99.9%), barium (> 99.0%), aluminium (> 99.9%) and calcium (99.5%). The melt's temperature was kept constant and it was stirred at 720°C for ten minutes. For comparison, two creep-resistant

magnesium alloys AE42 and MRI230D were selected for compression creep tests. All alloys were cast in rectangular moulds preheated to 300°C. To avoid turbulence while filling the moulds, a rising cast process was used. Nominal compositions of the alloys are given in Table 1. After filling, the mould was cooled with water. Optical and electron microscopy was used for the microstructural analysis. For SEM, a ZEISS Ultra 55 equipped with an energy-dispersive X-ray analysis (EDX) system at an accelerating voltage of 15 kV was used. Cylindrical specimens of 6 mm diameter and 15 mm length were prepared for compression creep tests by electrical discharge machining. The creep tests were performed with an ATS Lever testing system at constant temperatures and constant stresses.

Table 1: Nominal composition of the three alloys in wt.-%.

Alloy	Al	RE*	Mn	Ba	Ca	Sr	Sn	Mg
AE42	4	2	0.3	--	--	--		bal.
MRI230D	6-7	--	<0.3	--	2.1	0.3	0.84	bal.
DieMag422	4	--	--	2	2	--		bal.

*RE: Rare-earth elements, usually a mixture (Mischmetal)

Results and Discussions

Microstructure: The newly developed magnesium alloy DieMag422 was cast in a semi-conventional casting process with medium cooling and solidification speeds. The microstructure that formed can be seen Fig. 1.

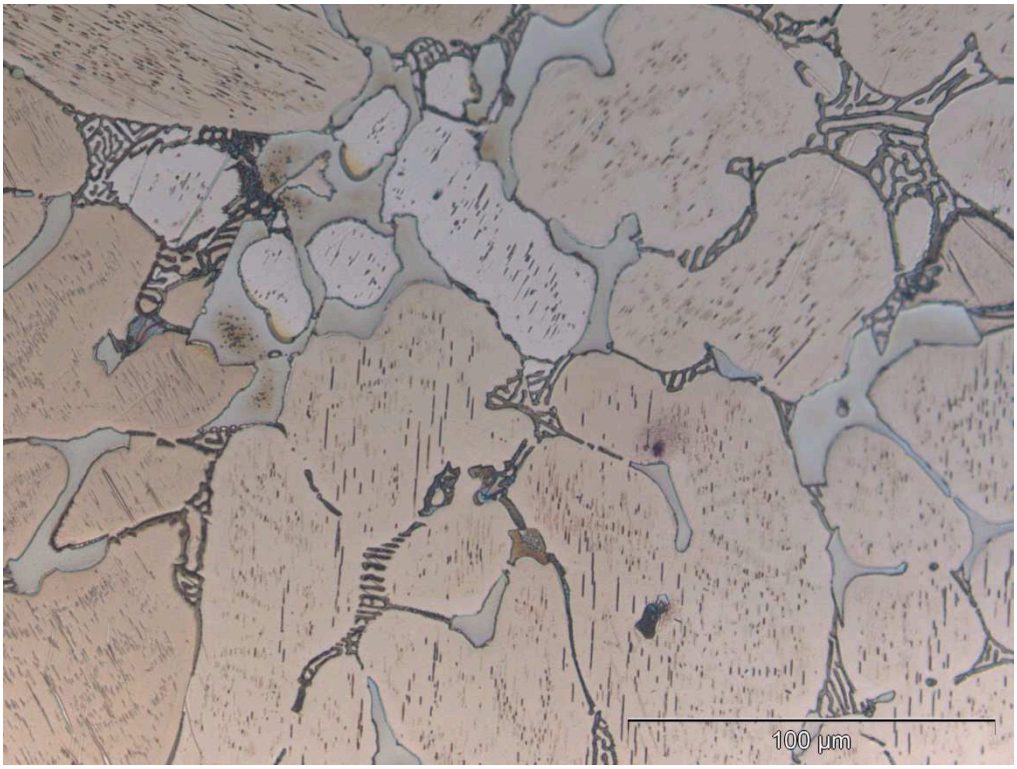

Fig. 1: Microstructure of cast magnesium alloy DieMag422

Two different morphologies and types of particles can be identified in the optical micrograph, a lamellar phase and a blocky phase. An EDX line scan performed [15] shows that the lamellar phase contains only Al and Ca, but no Ba or Mg. The ratio of Al to Ca is close to two, shown by a

statistical analysis at twenty points. Thus it can be concluded that the phase is Al_2Ca. The blocky phase is ternary, containing Mg, Al and Ba with very little Ca. A statistical investigation using twenty EDX point-analyses resulted in a composition of 80.2±1.1% Mg, 11.5±0.8% Al, 7.5±0.5% Ba. The blocky phase therefore has a structural formula $Mg_{21}Al_3Ba_2$ based on these quantitative results [15].

Creep Behaviour: Creep curves of the compression creep tests performed at 175°C and 100 MPa applied stress can be seen in Fig. 2. Fig. 2a shows the classic creep curve of creep deformation over time and Fig. 2b shows the first derivative of Fig. 2a, which is the creep rate over time. The minimum of each curve in Fig. 2b represents the minimum creep rate of each creep test.

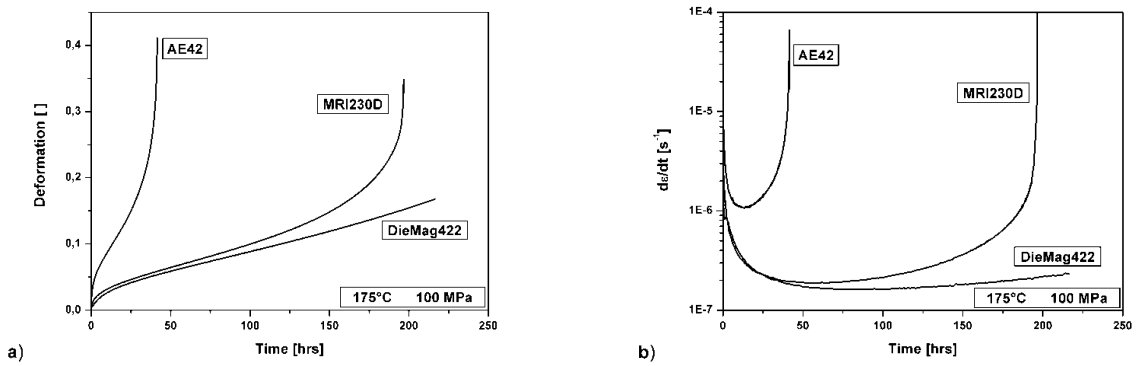

Fig. 2: Creep curves of tests performed at 175°C and 100 MPa, a) deformation over time and b) creep rate over time.

The dependence of the minimum creep rate $\dot{\varepsilon}_s$ on temperature T and applied stress σ is given by the Norton-Arrhenius-Equation (Eq. 1)

$$\dot{\varepsilon}_s = \frac{ADGb}{kT}\left(\frac{\sigma}{G}\right)^n \qquad \text{(Eq. 1)}$$

where A is a material dependent constant, G the shear modulus, b the Burgers vector, k the Boltzmann constant and n the stress exponent. The stress exponent n gives information about the rate-controlling deformation mechanisms during creep. The diffusion coefficient D can be expressed as:

$$D = D_0 \cdot \exp\left[-\frac{Q_c}{RT}\right]. \qquad \text{(Eq. 2)}$$

D_0 is the frequency factor and Q_C the apparent activation energy for creep. The stress exponent n can be determined by plotting the minimum creep rates in a double logarithmic creep rate and stress field. Fig. 3a-d shows these plots at the different temperatures under which the creep tests were performed. The stress exponent value n varies between 7.4 and 11.7 for different alloys at the tested temperatures. At all tested temperatures, the conventional magnesium alloy AE42 shows the highest minimum creep rates and therefore the worst creep resistance. At lower stresses, DieMag422 beats MRI230D at all temperatures, only at very high stresses is there a better performance by MRI230D.

The existence of a threshold stress (or back stress) σ_{thr} was described for precipitate and particle-hardened alloys. The interaction between dislocations and precipitates is assumed to be the origin of threshold stress, but different explanations exist for the details of this, including the additional stress that is needed to bow the dislocation between the precipitates, called Orowan

stress [16], the stress required to detach a dislocation from an obstacle [17, 18] and the additional back stress required to climb over an obstacle [19]. To introduce threshold stress σ_{thr} into the calculation, Eq. 1 is usually modified so that the effective stress σ_{eff} replaces the applied stress σ:

$$\sigma_{eff} = \sigma - \sigma_{thr} \quad \text{(Eq. 3)}$$

so giving Eq. 4 as

$$\dot{\varepsilon}_s = \frac{ADGb}{kT}\left(\frac{\sigma_{eff}}{G}\right)^{n_t} \quad \text{(Eq. 4)}$$

Here n_t is the true stress exponent, which is calculated based on the concept of a threshold stress. Li and Langdon found a method to calculate the threshold stress [20]. It is also described [15] for these materials. Threshold stresses decrease with increasing temperature (see Table 1). DieMag422 resulted in the highest threshold stresses and AE42 the lowest. By this method, the plots of minimum creep rates over effective stress σ_{eff} give the true stress exponent n_t as seen in Fig. 4a-d. After applying the concept of threshold stress, the true stress exponents n_t are in a range that fits to the theoretical assumptions concerned with the deformation mechanisms. A value of n=3 is related to the viscous glide of dislocations, n=5 is related to dislocation climbing at high temperatures and n=7 to dislocation climbing at low temperatures.

Table 1: Threshold stress σ_{thr} of all alloys at the different test temperatures.

Alloys	Threshold stress σ_{thr} [MPa] at			
	150°C	175°C	200°C	240°C
AE42	45.9	36.6	29.5	19.1
MRI230D	54.1	42.0	30.5	18.3
DieMag422	56.2	51.1	43.1	23.0

AE42 alloy gives values of n_t between 3.8 and 6.6 under all temperatures and for this alloy dislocation climbing appears to be the rate-controlling deformation mechanism. Both the MRI230D and DieMag422 alloys show an increase of n_t with increasing temperature. For these alloys dislocation glide is apparently the rate-controlling mechanism at 150°C, whereas at higher temperatures it is dislocation climbing.

By plotting the temperature-normalized minimum creep rate over the shear modulus-normalized applied stress in Fig. 5a it can be seen that of all the tests the AE42 alloy exhibits the worst creep resistance and MRI230D is better, but DieMag422 is the best, especially at low stresses. In Fig. 5b the temperature-normalized minimum creep rate is plotted over the normalized effective stress and in the higher stress ranges a true stress exponent n_t close to 5 can be estimated. This agrees well with investigations into the creep response of AS21 alloy by Zhang [21].

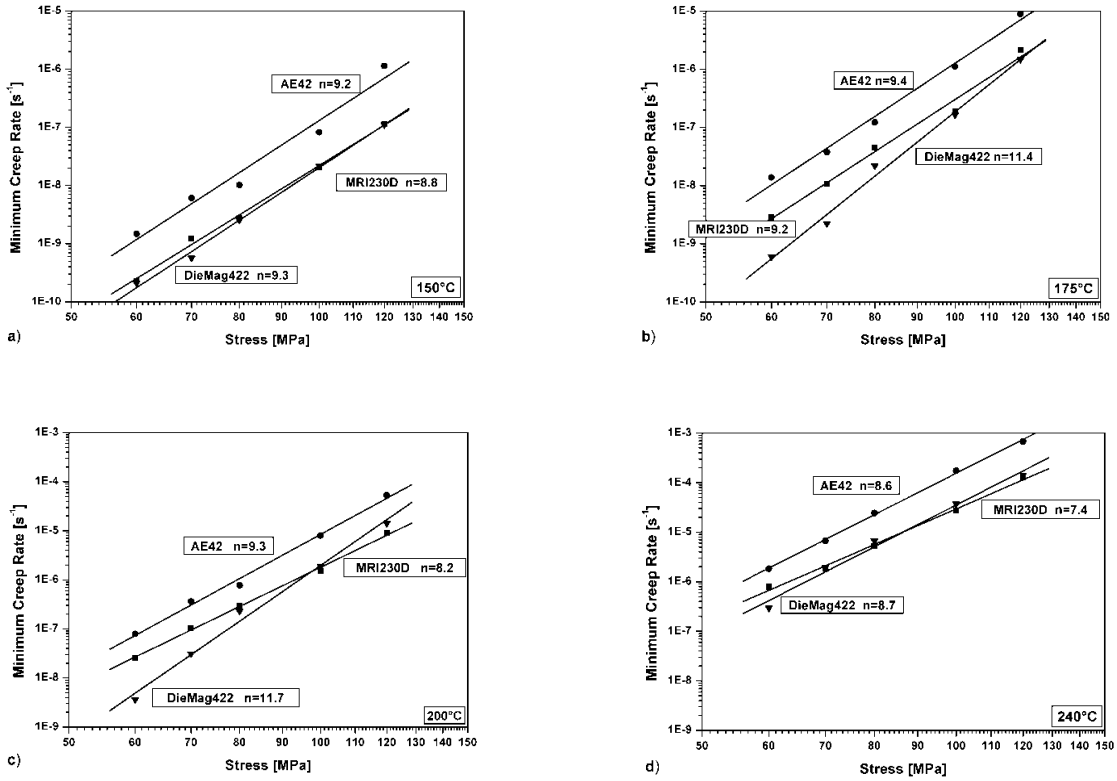

Fig. 3: Minimum creep rates over applied stress from creep tests at a) 150°C, b) 175°C, c) 200°C and d) 240°C.

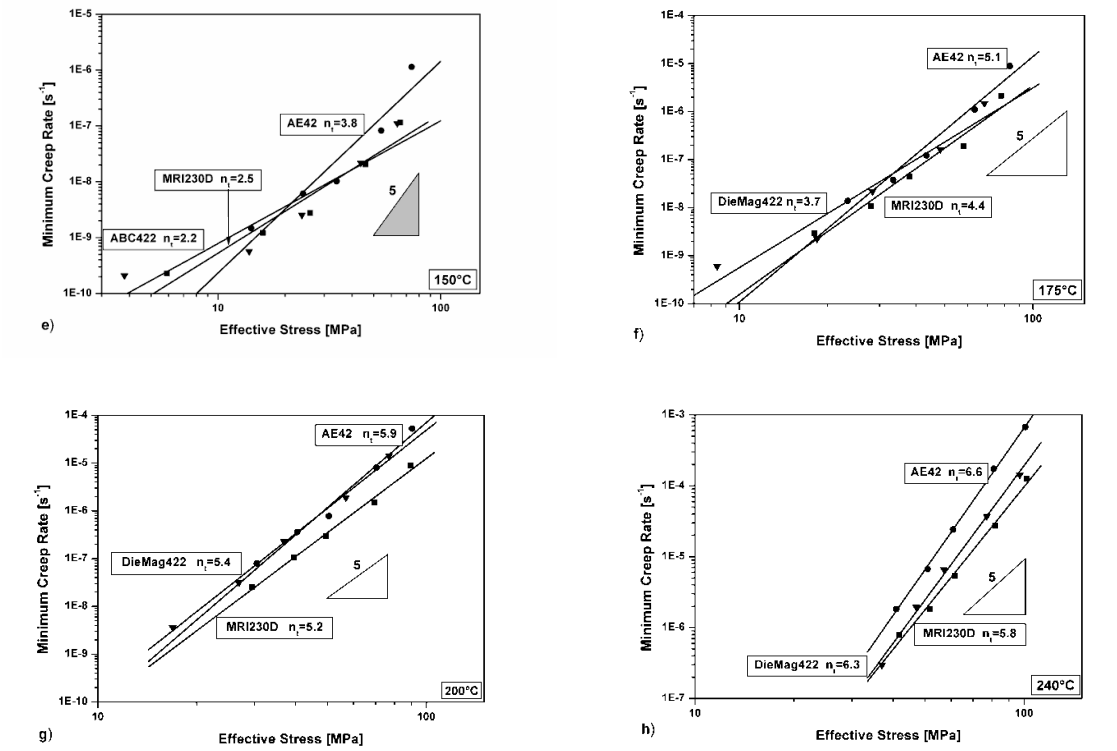

Fig 4: Minimum creep rates over effective stress from creep tests at a) 150°C, b) 175°C, c) 200°C and d) 240°C.

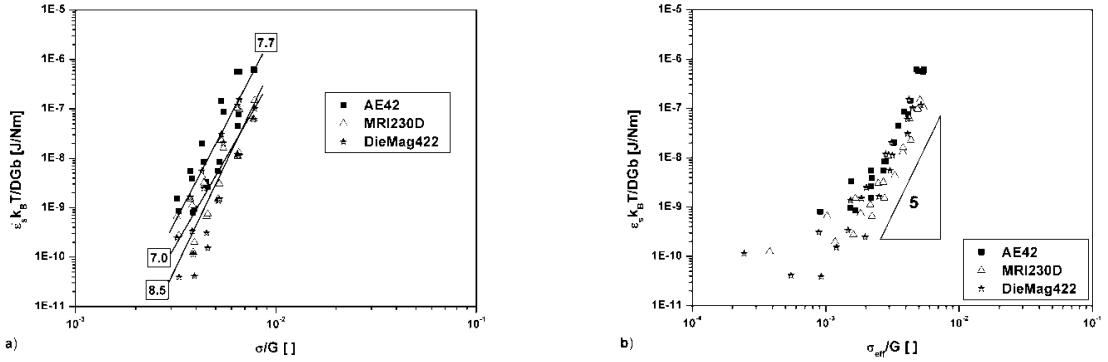

Fig. 5: Temperature-normalized minimum creep rate as a function of a) the shear modulus normalized applied stress, and b) the shear modulus normalized effective stress.

Summary

Two phases could be identified in the microstructure of magnesium alloy DieMag422. A lamellar phase identified as Al_2Ca and a blocky phase that is $Mg_{21}Al_3Ba_2$. Minimum creep rates of tests with DieMag422 were compared with of the same tests with AE42 and MRI230D, which are two commercial creep-resistant magnesium alloys for HPDC applications. It was found that the threshold stresses of each alloy decreases with increasing temperature, but DieMag422 shows the highest threshold stress, which results in excellent creep resistance. True stress exponents close to 5 indicate the rate-controlling deformation mechanisms are dislocation glide at lower temperatures and dislocation climb at higher temperatures. Other investigations [22] have already proven the die castability of magnesium alloys with various levels of barium content.

References

[1] W. Klemm, F. Dinkelacker: Z. Anorg. Chem. 255 (1947) 2–12.

[2] Zeek, (Ph.D.thesis): The system barium-magnesium and the structure of BaMg2, 1956, Syracuse University.

[3] K.P. Anderko: Trans. AIME 209 (1957) 612–616.

[4] Z. Yang, J. Du, B. Wen, C. Hu, R. Melnik: Intermetallics 32 (2013) 156–161.

[5] X. Ren, C. Li, Z. Du, C. Guo, S. Chen: Int. J. Mater. Res. 104 (4) (2013) 358–363.

[6] E. Alberti: Z. Metallkd. 26 (1) (1934) 6–9.

[7] M. Iida: J. Jpn. Inst. Met. 17 (1953) 632–634.

[8] G. Bruzzone, F. Merlo: J. Less-Common Met. 39 (1975) 1–6.

[9] R.P. Elliot, F.A. Shunk: Bull. Alloy Phase Diagrams 2 (3) (1981) 351–353.

[10] S. Srikanth, K.T. Jacob: Z. Metallkd. 82 (1991) 675–679.

[11] S. Srikanth, K.T. Jacob: Metall. Trans. B22B (1991) 607–616.

[12] V.P. Itkin, C.B. Alcock: J. Phase Equilib. 14 (4) (1993) 518–524.

[13] M. Regev, A. Rosen, M. Bamberger: Metall. Mater. Trans. A 32A (2001) 1335–1345.

[14] D. Wenwen, S. Yangshan, M. Xuegang, X. Feng, Z. Min, W. Dengyun: Mater. Sci. Eng. A356 (2003) 1–7.

[15] H. Dieringa, Y. Huang, P. Wittke, M. Klein, F. Walther, M. Dikovits, C. Poletti: Mat. Sci. Engin. A 585 (2013) 430-438.

[16] E. Orowan, In: M. Cohen (Ed.), Dislocation in Metals, AIME, 1954.

[17] E. Arzt, D.S. Wilkinson: Acta Metall. 34 10 (1986) 1893-1898.

[18] E. Arzt, J. Rösler: Acta Metall. 36 4 (1988) 1053-1060.

[19] E. Arzt, M.F. Ashby: Scr. Metall. 16 (1982) 1285-1290.

[20] Y. Li, T.G. Langdon: Scr, Mater, 36 12 (1997) 1457-1460.

[21] P. Zhang: Scr. Mat. 52 (2005) 277-282.

[22] H. Dieringa, D. Zander, M.A. Gibson: Mat. Sci. Forum 765 (2013) 69-73.